

Personal Identification Based on Blood Vessels of Retinal Fundus Images

Keisuke Fukuta*^a, Toshiaki Nakagawa^a, Yoshinori Hayashi^b,
Yuji Hatanaka^c, Takeshi Hara^a, Hiroshi Fujita^a

^aDepartment of Intelligent Image Information, Graduate School of Medicine, Gifu University,
1-1 Yanagido, Gifu-shi, Gifu 501-1194, Japan

^bTAK Co., Ltd., 4-35-12 Kono, Ogaki-shi, Gifu 503-0803, Japan

^cDepartment of Electronic Control Engineering, Gifu National College of Technology,
2236-2 Kamimakuwa, Motosu-shi, Gifu 501-0495, Japan

ABSTRACT

Biometric technique has been implemented instead of conventional identification methods such as password in computer, automatic teller machine (ATM), and entrance and exit management system. We propose a personal identification (PI) system using color retinal fundus images which are unique to each individual. The proposed procedure for identification is based on comparison of an input fundus image with reference fundus images in the database. In the first step, registration between the input image and the reference image is performed. The step includes translational and rotational movement. The PI is based on the measure of similarity between blood vessel images generated from the input and reference images. The similarity measure is defined as the cross-correlation coefficient calculated from the pixel values. When the similarity is greater than a predetermined threshold, the input image is identified. This means both the input and the reference images are associated to the same person. Four hundred sixty-two fundus images including forty-one same-person's image pairs were used for the estimation of the proposed technique. The false rejection rate and the false acceptance rate were $9.9 \times 10^{-5}\%$ and $4.3 \times 10^{-5}\%$, respectively. The results indicate that the proposed method has a higher performance than other biometrics except for DNA. To be used for practical application in the public, the device which can take retinal fundus images easily is needed. The proposed method is applied to not only the PI but also the system which warns about misfiling of fundus images in medical facilities.

Keywords: retinal fundus image, identification, biometrics, blood vessel extraction, similarity

1. INTRODUCTION

Recently, several systems such as personal computers, cellular phones, automatic teller machines (ATM), and entrance and exit management systems have begun using automatic personal identification (PI). These systems are exposed to security attacks such as password and encryption key cracking and spoofing, and it is important to enhance security procedures to protect personal information. Therefore, biometric technologies, which identify individuals based on unique physiological and behavioral characteristics, have been implemented instead of conventional identification methods such as passwords and personal identification number (PIN) codes [1]-[5]. Biometric identification compare newly entered data (input data) with stored data (reference data) in database as well as the conventional identification methods. The ideal biometric system must be easy to use, fast in calculation, non-invasive for humans, convenient to the user, and socially acceptable. However, when certain equipment or a facility requires tight security, biometric solutions must prioritize the minimization of the risk of stolen personal identity information and high recognition accuracy over the convenience of implementation. Biometrics using retinal recognition is one of the most suitable methods for such situations. A relatively bulky device is required for stably obtaining biometric information from the retina. However, in

*Corresponding author information: E-mail: keisuke@fjt.info.gifu-u.ac.jp, Telephone: +81-58-230-6519

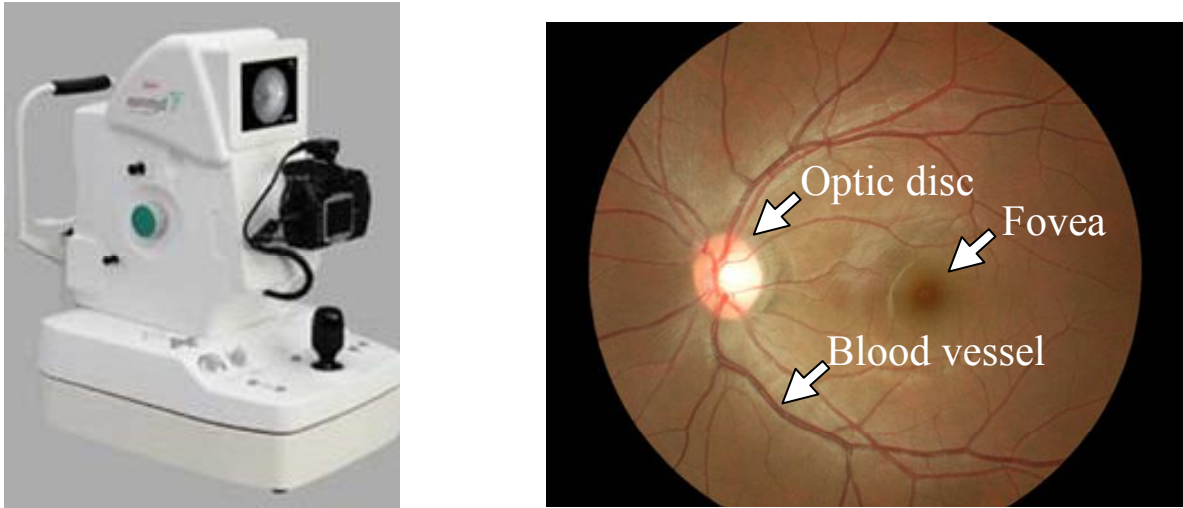


Fig.1 An example of the retinal fundus camera and retinal fundus image.

1935, Simon and Goldstein [6] discovered that the blood vessels (BVs) in the retina are unique to each individual; because of these characteristics, such systems can potentially be used for highly accurate personal recognition. Moreover, since the retina is within the human body, the pattern of retinal BVs remains stable for a long time except in the case of a disease, further, this pattern cannot be replicated by a third person. The fundus camera, which can capture photographs of the retina, is used in medical fields to diagnose diseases such as diabetic retinopathy and glaucoma. An example of a retinal fundus camera and photograph of the retinal fundus are shown in Figure 1. The fundus camera illuminates the retina by photoflash transmitted through the pupil and the image of part of the intraocular tissue such as BVs, fovea (the small spot in the retina where vision is keenest), and optic disc (OD, the head of the nerve to the eye) is acquired without any mydriatic drug. The retinal fundus image captured by the fundus camera contains information that is richer than that in a conventional vascular image pattern acquired from a small area of the retinal fundus because the former covers a relatively large area with color information in two dimensions. Therefore, it is considered that the retinal fundus image is useful for high-accuracy PI. The retinal fundus is the portion of the inner eye that can be seen during an eye examination by looking through the pupil [7].

This paper proposes a method that focuses on the BV configuration in the fundus image. By employing the BV region extracted from the fundus image for calculating the similarity between an input image and reference images, our identification system should produce a better result because the configuration of the BVs has individual characteristics as opposed to some other regions in the fundus image.

2. MATERIAL

The outline of the proposed method is shown in Figure 2. Four hundred sixty-two fundus images which comprise 41 image pairs for same-person were used in this work. These images were acquired using two different fundus cameras (camera A, camera B). In the camera A, four hundred fundus images which comprise 10 image pairs for same-person were used. In the camera B, sixty-two fundus images which comprise 31 image pairs for same-person were used. The field-of-view (FOV) coverage was 45°. The FOV was of a circular form and was truncated at both the top and the bottom. The image was stored in a compressed JPEG format. The fundus images were obtained from the subjects' left and right eyes, and they were approximately fovea centered by the fixation of the eye position using an internal light-emitting diode.

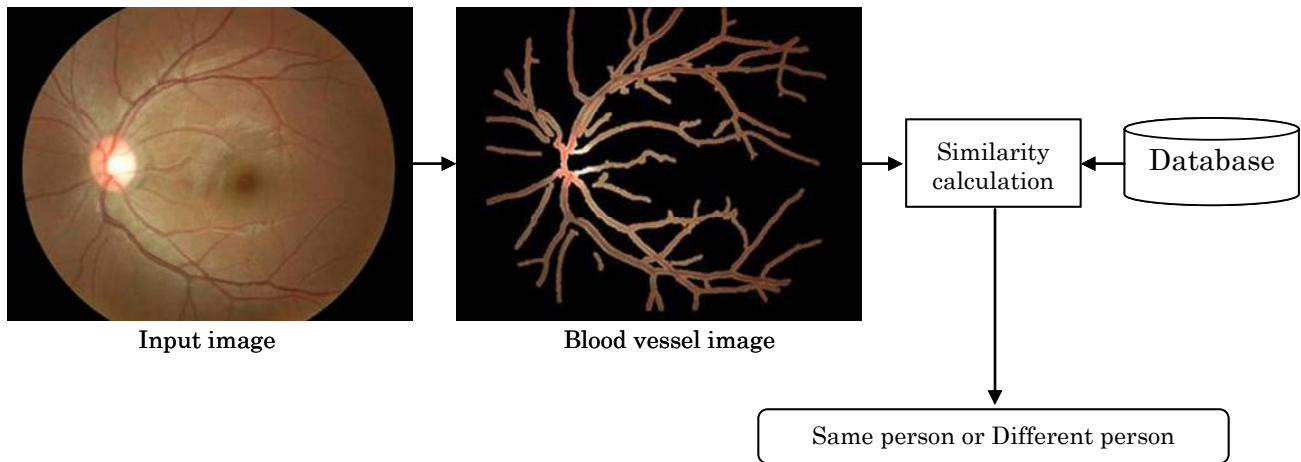


Fig.2 Outline of whole process in the PI.

As a preparation for capturing the fundus image, the alignment between the eye and the fundus camera was performed manually. The alignment was performed by overlapping two bright spots at two marks on the camera's monitor while bringing the objective closer to the subject's eye. An operator used a joystick for an in-out and left-right motion in order to manually perform the alignment. Additionally, the axial lengths of the eyes are different from each other. Therefore, although these were not significantly different, the magnifications of the fundus images were not exactly the same. The operator also adjusted the focus manually by tweaking the dial on the camera. As a result, a sharp focus was not achieved due to technical errors in some images. However, the defocus blurs became hardly noticeable due to the reducing process of the image matrix size.

3. METHODOLOGY

3.1 Overall scheme for personal identification using retinal fundus images

The proposed identification procedure compares an input fundus image with reference fundus images in the database. The flowchart of the proposed method is shown in Figure 3. In the first OD detection step, this step needs the BV image and the BV erased (BVE) image. The BV region was extracted from the input image by using morphological operations and thresholding, and the BV image was generated [8], [9]. To erase the BV region from the input image, the pixel values of the BV region in the input image were replaced by the average intensity of the pixels surrounding the BV using the input image and the BV image, and the BVE image was generated. The position of the OD in the input image was determined based on histogram analysis using the pixel values of the BVE image. Results of the BV extraction process and erasing BV process are shown in Figure 4. The BV image was also used to improve the accuracy of OD detection. The process mentioned above was applied to the reference image as well. Subsequently, in the second and third steps, the translational and rotational displacements between the input and reference images were compensated by the iterative execution of the same procedures. The original images were adopted in the displacement compensation processes in order to perform the registration between not only the same person's images but also different person's images. Finally, in the fourth step, the similarity between the resulting displacement-compensated images was calculated based on the cross-correlation coefficient of the pixel values of the BV images. In order to consider the distortion effects of the camera lens, the BV image of the input image was divided into equal square regions and the averaged cross-correlation coefficients calculated from each pattern-matched region was defined as the similarity.

The following subsections present a detailed description of the techniques used for OD detection, the registration between input and reference images, and the calculation of similarity in the proposed method.

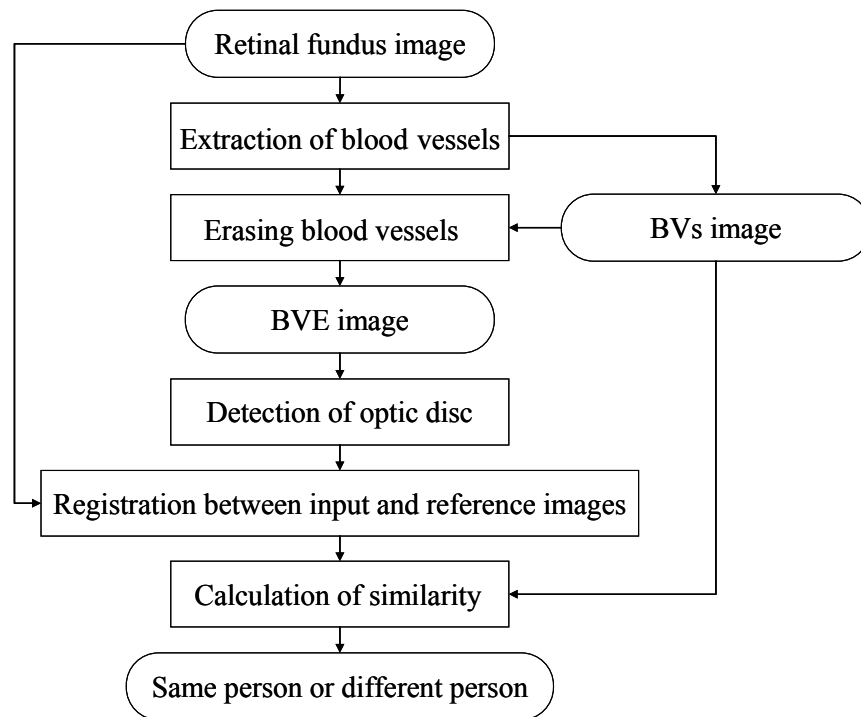


Fig.3 Flowchart of similarity calculation for PI of retinal fundus image.

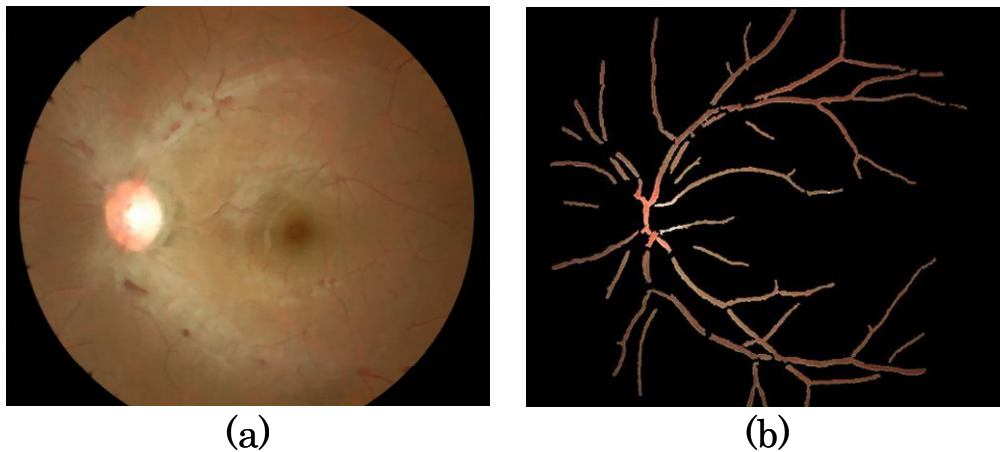


Fig.4 Results of BV extraction process and BV erasing process. (a) BVE image, and (b) BV image.

3.2 Detection of optic disc

The OD region has relatively high pixel values in three channels (R, G, and B components) in the fundus images. Moreover, the size of the OD is approximately 1.5 mm in horizontal diameter and individual variations of the OD do not vary significantly. Because of these reasons, the P-tile method can be applied to define a threshold for an approximate extraction of the ONH region [10].

The BVs running on the surface of the OD interfered with the correct extraction of the OD region in the P-tile thresholding operation. In order to solve this problem, the extraction of the OD region was performed by using the BVE images.

The contour of the OD appears clearly in the R component image of many fundus images, but there were some cases in which the contours of the OD were blurred or invisible even in this. Therefore, the P-tile method was applied to the three component images, and the region in which more than one component image overlapped was determined as an OD candidate. The value of “*P*” in the P-tile thresholding operation was experimentally set to a value slightly greater than the average area of the OD.

When more than one candidate region was extracted, the candidate region with the maximum area was selected as the OD region. Additionally, the candidates were estimated by computing their circularity, which is defined as: $circularity = 4\pi \times area/perimeter^2$. Subsequently, the candidates having circularity values less than a predetermined value were excluded. After preliminary experiments, we set the threshold value for the circularity to 0.45. The coordinate of the OD region was determined at the gravity point of the OD region extracted from the images. The extraction process of the OD region was implemented in the images that were reduced to 1/4th of the inputted fundus images.

3.3 Registration between input and reference images

In rare cases, the input image perfectly matches the reference image. Displacements almost always occur between the input and reference images and these adversely affect the result of the similarity calculation. Due to the occurrence of displacements, the similarity becomes low even in the case of the same persons' images; consequently, the accuracy of PI decreases. Therefore, the displacements need to be compensated before the similarity calculation. The registration includes translational and rotational displacements.

The registration of translational displacements was implemented by the template matching technique using the template image including the OD region of the input image. The template image was obtained from a 100 × 100 pixel square centered at the central coordinate of the OD region. The similarity between the template image and the block area in the reference image was calculated, and then the block area having the maximum value was recognized. Next, the entire input image was shifted to the best matching position. The similarity was defined by the cross-correlation coefficient of the RGB pixel value. In order to reduce the calculation time, the search area in the reference image for finding the best matching position was limited to a 100 × 100 pixel square centered at the central coordinate of the OD region of the reference image.

In order to measure the amount of rotational displacement, the similarity between the input and reference images was calculated every time when the input image was rotated from -5° to 5° with a 1° interval around the coordinate of the OD region, and then the rotational position having the maximum value was recognized. Next, the input image was rotated to the best matching position. The similarity was defined by the cross-correlation coefficient of the RGB pixel value. Note that the pixels in region outside the FOV were excluded from the similarity calculation.

3.4 Calculation of similarity

The PI was implemented based on a similarity defined by the cross-correlation coefficient of the RGB pixel value between the input and reference images. In other words, when the similarity was greater than a predetermined threshold, the input image was identified as the same person's image. Conversely, when the similarity was less than or equal to the threshold, the input image was recognized as a different person's image. The pixels used in the similarity calculation were not sampled from the entire region of the FOV but from a 360 × 360 pixel square centered at the central coordinate of the OD region. The calculation area is limited because the difference in the pixel values between the input and reference images tends to be large, especially near the margin of the FOV, and the regions will adversely affect the accuracy of PI.

The decrease in identification accuracy can be partly attributed to radial lens distortion. Many techniques have been reported for correcting the lens distortion in a photographic image. In this study, we applied the simple method described below for lens distortion correction. The 360 × 360 pixel square was divided into 36 smaller squares with a size of 60 × 60 pixels each. Next, template matching was performed on the small squares, and then the average of the similarities of each small square was defined as the similarity between the input and reference images. In this process, the smaller squares were moved at most 5 pixels to the left, right, up, and down from their initial location.

4. EXPERIMENT AND RESULT

The similarities between all fundus images used in this study were calculated. When one image was selected from 462 images as the input image, another 461 images were used as the reference images. Hence, the similarities of 106,491 combinations were obtained.

Figure 5 shows two histograms of the similarities between the same and different person's images in the proposed method. A statistically significant difference was found between the two groups ($p < 0.001$).

There are two important specifications in any biometric system. One is the false rejection rate (FRR) and the other is the false acceptance rate (FAR). FRR denotes the probability that an authorized person is rejected access and FAR denotes the probability that a non-authorized person is accepted as an authorized person. Figure 6 shows the relation between FRR and FAR obtained from the distribution of the similarity. In proposed method, FAR was $4.3 \times 10^{-5}\%$ when the FRR was $9.9 \times 10^{-5}\%$.

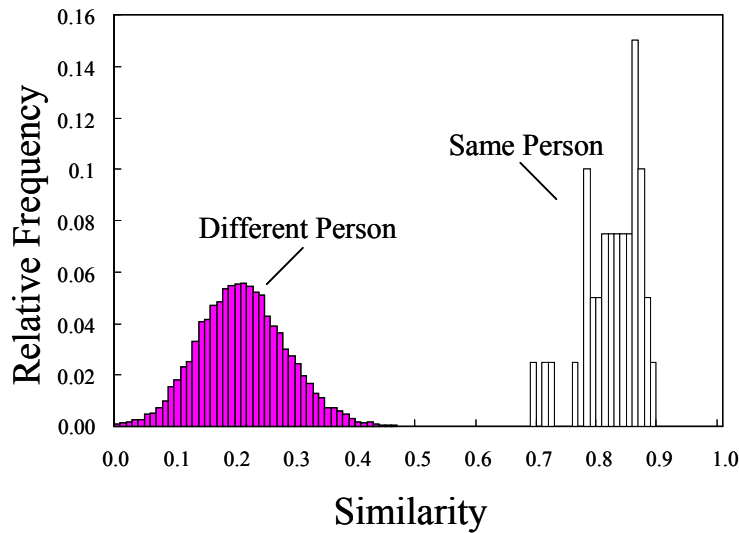


Fig.5 The Result of calculation of similarity in the proposed method.

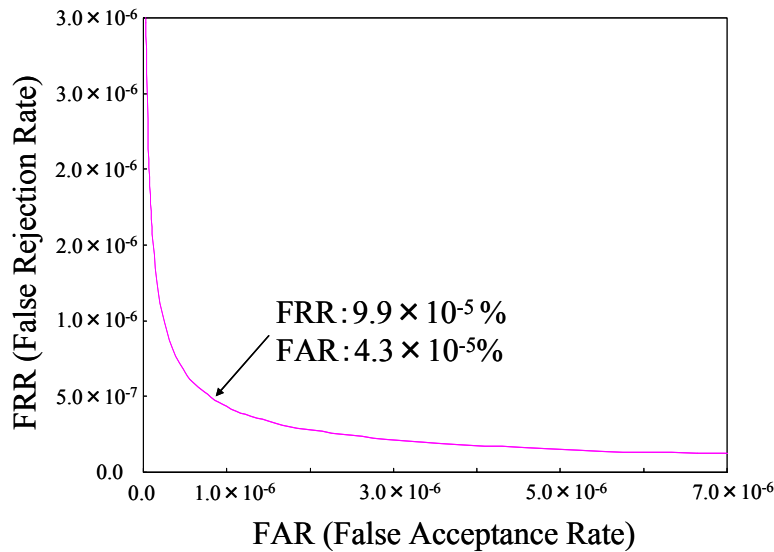


Fig.6 The relation between FRR and FAR.

5. DISCUSSION

The similarities of the same person's image pairs were significantly larger than the similarities of a different person's image pairs. The results confirm the individual characteristics of the BV configuration and its usefulness in PI.

Figure 7 shows the distribution of the similarity that is calculated using the original images. It shows that the two distribution functions overlap in a relatively wide range. Figure 8 shows an example of the improved case in which the similarity between the same person's images (0.432) was lower than that in a different person's images (0.463) when using the original images. These results indicate that the BV images effectively improve the similarity between the input and reference images by enhancing the individual characteristics in the fundus image. Therefore, we believe that the similarity calculation using the BV region is effective in PI.

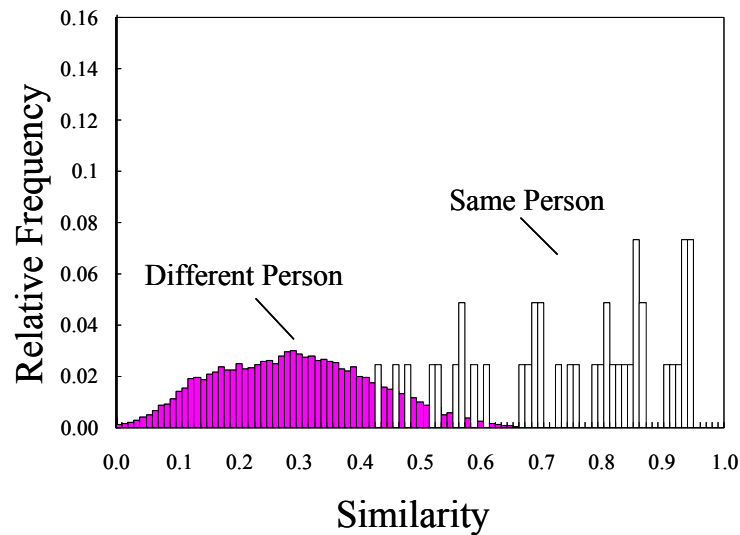


Fig.7 The distribution of the similarity using the original images.

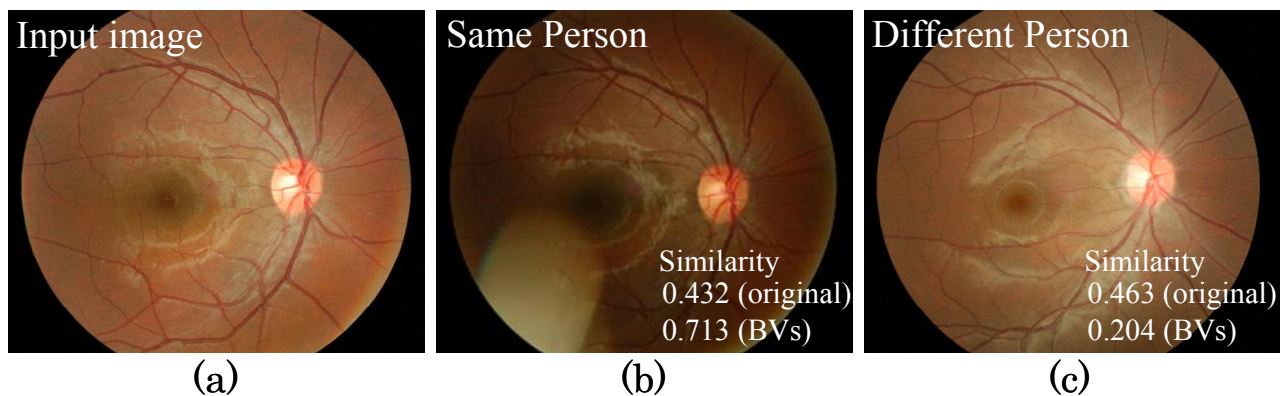


Fig.8 Compensation of similarity between original and BV images. (a) input image, (b) same person's image [Similarity = 0.432 (original), 0.713 (BVs)], (c) different person's images [Similarity = 0.463 (original), 0.204 (BVs)].

Table 1 The comparison with other biometrics.

	False Acceptance Rate	False Rejection Rate
DNA	$1.0 \times 10^{-13} \%$	Less than measurement error
Proposed method	$4.3 \times 10^{-5} \%$	$9.9 \times 10^{-5} \%$
Iris	$8.3 \times 10^{-5} \%$	$1.0 \times 10^{-1} \%$
Fingerprint	$2.0 \times 10^{-4} \%$	$5.0 \times 10^{-2} \%$
Face	1%	1%
Voiceprint	3%	3%

The FRR and FAR of the proposed method indicate that the method achieves high performance. The comparison with other biometrics is shown in Table 1. The proposed method was better than other biometrics except for DNA biometrics. However, it is necessary to compare this method with other PI techniques for a larger dataset.

We found that the BV configuration was effective in calculating the similarity for PI using retinal fundus images. However, when the algorithm includes the segmentation process of blood vessel regions, it could be assumed that the identification accuracy depends on the result of segmentation. Therefore, an improvement in the accuracy of BV extraction is expected to improve the accuracy and robustness of identification. Moreover, a device that can easily and stably capture fundus images with clear and high contrast is fundamental to the practical implementation of this method in common situations. We expect that the proposed method may have applicability not only in tight security situations but also in a picture archiving and communication system (PACS) for detecting filing errors [11].

6. CONCLUSION

This paper has presented a new PI method by using the BV regions of retinal fundus images. The proposed method has FRR and FAR values of $9.9 \times 10^{-5} \%$, $4.3 \times 10^{-5} \%$, respectively. Therefore, it is considered that this technique is useful for PI.

The following topics are considered for further research. The identification method should be applied to images having abnormalities or images exhibiting yearly variations in the retina. The compensation of the displacement between the images should be implemented with higher accuracy and greater robustness.

ACKNOWLEDGMENT

This study was supported in part by a grant for the Knowledge Cluster Creation Project from the Ministry of Education, Culture, Sports, Science and Technology, Japan under the heading "Gifu-Ogaki Area: Robotics Pioneering Medical Care Cluster." The authors would like to acknowledge the contribution of Dr. T. Yamamoto of the Graduate School of Medicine, Gifu University.

REFERENCES

1. Biometrics: Personal Identification in a Networked Society, A. K. Jain, R. Bolle, and S. Pankanti, eds., Springer-Verlag New York Inc (C),1999.

2. S. Prabhakar, S. Pankanti, and A. K. Jain, "Biometric recognition: Security and privacy concerns," *IEEE Security and Privacy*, vol. 1, no. 2, pp. 33–42, Mar, 2003.
3. A. K. Jain, A. Ross, and S. Prabhakar, "An introduction to biometric recognition," *IEEE Trans. on Circuits and Systems for Video Technology*, vol. 14, no. 1, pp. 4–20, Jan, 2004.
4. K. Delac and M. Grgic, "A survey of biometric recognition methods," *Proc. of the 46th International Symposium Electronics in Marine, ELMAR-2004*, pp. 184–193, 2004.
5. A. K. Jain, A. Ross, and S. Pankanti, "Biometrics: A tool for information security," *IEEE Trans. on Information forensics and security*, vol. 1, no. 2, pp. 125–143, Jun, 2006.
6. C. Simon and I. Goldstein, "A New Scientific Method of Identification," *New York State Journal of Medicine*, vol. 35, pp. 901–906, 1935.
7. Spectacle World, "Dictionary of the eye," <http://www.spectacleworld.co.za/eyecare04.htm>
8. J. Serra, "Introduction to mathematical morphology," *Computer Vision, Graphics, and Image Processing*, vol. 35, no. 3, pp. 283–305, 1986.
9. S. R. Sternberg, "Grayscale morphology," *Computer Vision, Graphics, and Image Processing*, vol. 35, no. 3, pp. 333–355, 1986.
10. J. R. Parker, "Algorithms for Image Processing and Computer Vision," Wiley Computer Publishing, New York, 1997.
11. J. Morishita, S. Katsuragawa, K. Kondo, and K. Doi, "An automated patient recognition method based on an image-matching technique using previous chest radiographs in the picture archiving and communication system environment," *Medical Physics*, vol. 28, no. 6, pp.1093–1097, 2001.